Microstructure and Properties of Laser Cladding AlxFeCoCrNiMn High Entropy Alloy of Q345 Steel

Dongfang Yan[a], Chuanwei Shi[a]*, Jianyang Wang[b], Yuanbin Zhang[a], Junhua Sun[a], Yongbin Wang[a],

Peng Liu[a] 🆔

[a] Shandong Jianzhu University, School of Materials Science and Engineering, Jinan 250101, P. R. China.
[b] Huanghai Shipbuilding Co. LTD, Rongcheng 264309, P. R. China.

High entropy alloy is a multi-component alloy material with equal or near atomic number, which has excellent wear resistance and corrosion resistance. In this paper, AlxFeCoCrNiMn (x = 0,0.5,1.0,1.5) high entropy alloy cladding layer was prepared by laser cladding on Q345 steel plate. The phase structure, microstructure, hardness and wear resistance of the cladding layer were studied. The results show that the cladding layer of AlxFeCoCrNiMn alloy has good metallurgical bonding ability with Q345 steel. The cladding area is mainly columnar and equiaxed. The cladding layer of AlxFeCoCrNiMn alloy is mainly composed of BCC + FCC solid solution phase, which is caused by the addition of Al element under the high entropy effect. Al element promotes the formation of BCC phase structure. With the increase of Al element, the hardness of cladding layer increases. The hardness of $A_{1.0}$ cladding layer is 670HV, which is close to three times of Q345 steel. When Al (x = 1.0), the hardness of the cladding layer is the highest, and it also shows better wear resistance with lower friction and wear loss.

Keywords: *high entropy alloy, cladding layer, microstructure, hardness.*

1. Introduction

High entropy alloy is a new type of alloy with excellent properties developed in recent years. It has five or more main elements, each of which is between 5% and 35%[1-3]. As a new type of multi-principal alloy material[4,5], it breaks the traditional design concept of a single principal element of alloy, and creates a new idea for the field of alloy design. High entropy alloy is advantageous to the formation of simple solid solution phase due to its high entropy effect, and at the same time, it prevents the formation of complex intermetallic compounds during solidification process, and has good metal properties[6]. Previous studies have shown that the cladding layer of high entropy alloy has high microhardness, high oxidation resistance and good corrosion resistance[7,8]. Therefore, high entropy alloy has a wide range of prospects in the surface modification of materials.

Q345 steel is widely used in bridge, ship, vehicle and pressure vessel[9]. Laser cladding is an important method of material surface modification. It is a kind of cladding layer with different composition and performance on the surface of the substrate by using high energy density laser beam to melt the alloy with different composition and performance quickly. The laser cladding process parameters determine the properties of the cladding layer to a large extent[10,11]. In order to reduce the crack rate of laser cladding material effectively, the quality of the composite cladding material must be improved. Laser cladding can control the thickness and has strong metallurgical bonding ability. It shows the

superiority in improving the wear resistance of the material. Because of the large atomic radius, Al element will produce lattice distortion, increase the confusion of entropy value of high entropy alloy, promote the formation of BCC single solid solution phase, enhance the solid solution strengthening effect of solid solution, and improve the hardness, wear resistance and oxidation resistance of high entropy alloy; Laser cladding of Alx system high entropy alloy cladding is one of the hot spots in laser cladding of high entropy alloy. In addition, there are a lot of nickel and chromium in the alloy system, both of which can improve the corrosion resistance of HEAS[12]. In addition, the atomic size, electronegativity and valence electron concentration of different atoms in the design element are significantly different, which leads to lattice distortion, thus improving the hardness of HEAS[13,14]. Therefore, in view of the low strength and wear resistance of Q345 steel in some special environments, the laser cladding technology is used to prepare AlxFeCoCrNiMn (x=0, 0.5, 1.0, 1.5) high entropy alloy cladding layer on the surface of Q345 steel, so as to optimize the performance and prolong the service life.

Zeng et al.[15] used laser cladding to prepare AlxCoCrFeNi high entropy alloy cladding layer. It was found that with the increase of Al content, the microstructure grain of AlxCoCrFeNi high entropy alloy cladding layer was relatively coarse; The structure of $Al_{0.55}$CoCrFeNi alloy is columnar dendrite, and the gray area in dendrite is more than that of black area between dendrites; $Al_{0.75}$CoCrFeNi alloy is equiaxial amorphous structure; $Al_{1.25}$CoCrFeNi alloy is a typical amplitude

modulation decomposition structure, and the dendrite region is a typical amplitude modulation decomposition structure, and the alloy melt is converted into B2 and BCC phases from the melt at high temperature, and the following solidification bcc structure is formed between the dendrites; The cladding layer of FeCrNiCoCuAlx high entropy alloy was prepared on Q345 steel surface by laser cladding technology[16]. When Al was not added, the microstructure of the cladding layer was composed of gray equiaxed crystal and white grain boundary. When the Al element increased, the large white columnar structure such as branch and fishbone appeared gradually. The high entropy alloy cladding layer of AlCoCrFeNiTix was prepared on the surface of AISI1045 steel by laser cladding method[17]. The results show that the phase structure of the system is mainly composed of disordered BCC solid solution phase (Fe Cr) and ordered BCC phase (al Ni). Liu et al.[18] studied the microstructure evolution of AlCoCrFeNiTix alloy at different heat treatment temperatures. It was found that the cladding layer consists of BCC FeCr solid solution matrix, B2 Al-Ni precipitate and in situ TiC particle phase. After 900 °C heat treatment, it can be observed that the coarsening behavior of AlNi precipitates leads to the decrease of wear resistance. Cui et al.[19] and others studied the high temperature wear resistance of the coating of FeCoCrNiMnAlx. It was found that with the increase of Al content, the hardness and wear resistance increased. The Al element enhanced the high temperature wear performance of FeCoCrNiMnAlx cladding alloy and effectively improved the properties of 4Cr5MoSiV base metal.

2. Experimental

In this experiment, AlxFeCoCrNiMn (x refers to different mol) high entropy alloy cladding layers were prepared by laser cladding technology. Q345 steel is selected as the base material, and its chemical composition table is shown in Table 1. Q345 steel plate was cut into 10 cm × 10 cm ×10 cm. The sample was polished with angle grinder and polished with coarse sandpaper. The mixture of FeCoCrNiMn powder with 99.9% purity and equal mole ratio (1:1:1:1) and Al powder with different mole number were used for proportioning, as shown in Table 2. In the test, in order to meet the requirements of synchronous powder feeding, Al powder in spherical form was selected, and the particle size was guaranteed to be 200 mesh. Figure 1 is a photograph of the alloy powder under electron microscopy. The parameters of various elements selected in this experiment are shown in Table 3. AlxFeCoCrNiMn (x = 0, 0.5, 1.0, 1.5) powder was put into the mixer to mix well. Before laser cladding,

the powder was dried in drying oven for 3 hours at 100 °C. At the same time, the substrate was preheated at 200 °C for 20 minutes.

IPG YLS 10000 fiber laser processing system is used for laser cladding. The laser adopts synchronous powder feeding, and argon gas is used as protective gas during the experiment. The technological parameters of laser cladding are: laser power is 1000W, scanning speed is 10mm•s⁻¹, spot diameter is 3mm, shielding gas flow is 20L/min, powder feeding speed is 10g/min, and lap rate is 40%.

The laser cladding samples were cut into uniform small pieces by WEDM, polished by MPT-200 metallographic polishing machine, and electrolyzed with 10% oxalic acid solution for 10s. The microstructure of the cladding layer was observed by IE 200M optical microscope (OM), the surface microstructure of the cladding layer and the bonding zone between the side cladding layer and the substrate were analyzed by JXA-8530F scanning electron microscope (SEM), and the cladding layer was analyzed by energy dispersive spectrometer (EDS). The phase structure of the cladding layer was analyzed by X-ray diffraction (XRD) with Cu Ka radiation. The target material was copper target and the scanning range was 20 °~ 100°.The current is 30A and the voltage is 40kV. The microhardness of the cladding layer under 1.98N load and 10s residence time was studied by microhardness tester (HV). Use M2000 dry sliding friction and wear tester to test the wear of coating. Cut the sample into 31 pieces before the test 31×6.5×3mm in size, take three samples of each type, clean the coating with ultrasonic acetone, and weigh in the tray balance before the test. During the wear process, the pressure load is 50N, the spindle speed is 200r/min, and the standard
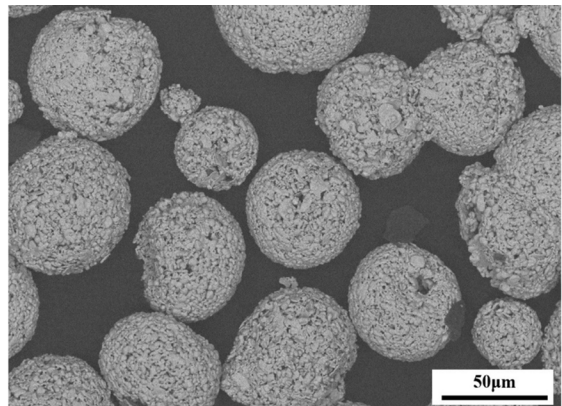

Figure 1. Morphology of alloy powder.

Table1. Element parameter table.

Elements	Atomic number	Crystal structure	Relative atomic mass	Atomic radius (Å)	Melting point (°C)	Electroneg-ativity (χ)	Density (g/cm³)
Al	13	FCC	26.98	1.82	660	1.66	2.702
Fe	26	BCC	55.84	1.72	1539	1.83	7.86
Co	27	HCP	58.93	1.67	1493	1.88	8.9
Cr	24	BCC	52.00	1.85	1863	1.66	7.22
Ni	28	FCC	58.96	1.62	1455	1.91	8.902
Mn	25	BCC	54.94	1.79	1244	1.53	7.44
B	5	Orthogonal	10.81	0.82	2076	2.04	2.34

used is GB3960. Clean and weigh every 1min. At the same time, the wear surface morphology was analyzed by scanning electron microscope, and the wear mechanism of the coating was analyzed by wear loss.

3. Results and analysis

3.1. Phase structure of alloys

The phase structure of AlxFeCoCrNiMn (x = 0,0.5,1.0,1.5) high entropy alloy cladding by laser cladding is analyzed by XRD. Figure 2 shows that there is only a simple diffraction peak in the cladding layer, and there is a strong peak accompanied by two weak peaks. With the increase of Al content, the peak with the highest diffraction intensity shifted significantly to the right. The results show that with the increase of Al content, the alloy undergoes displacement solution and lattice distortion. According to the literature report, only the chaos degree $\Omega \geq 1.1$ or the atomic radius difference $\delta \leq 6.6\%$ can form a stable solid solution phase. Calculate the chaos degree and atomic radius difference of the alloy cladding layer according to the following formulas.

$$Tmix = ci\% * Tx \qquad (1)$$

$$\Delta Hmix = \sum_{i \neq j} 4cicj\Delta Hij \qquad (2)$$

$$\Delta Smix = -R \sum_{i=1}^{n} ci \ln ci \qquad (3)$$

$$\Omega = \frac{Tmix\Delta Smix}{|\Delta Hmix|} \qquad (4)$$

$$\delta = \sqrt{\sum_{i=1}^{n} ci \left[1 - ri / \left(\sum_{i=1}^{n} ciri \right) \right]^2} \qquad (5)$$

In the formulas, T_{mix} is the mixing melting point; T_x is the melting point of the element; c_i is the atomic ratio; ΔH_{mix} is the mixing enthalpy; ri is the atomic radius; $\Delta Smix$ is the mixing entropy; R is the general gas constant. R=8.314J•mol⁻¹•K⁻¹;Ω is the degree of chaos; δ is the atomic radius difference. The alloy parameters can be calculated by the formula and Table 1 and Table 4, as shown in Table 5. The results show that the Ω of alloy powder is above 1.1, δ Both are below 6.6%, so the replacement solid solution

of Al$_x$FeCoNiCrMn high entropy alloy will occur, and only a single FCC or BCC phase solid solution will be formed.

Compared with the standard PDF card, the diffraction peak in the alloy mainly consists of one main peak (200) and two weak peaks (111) and (220). After comparison with JADE6.0, it is found that the Al$_0$ cladding layer only presents one FCC phase. With the increase of Al content, the Al$_{0.5}$ cladding layer has no change, and it is still a single FCC solid solution phase. This is because Fe, Co, Cr, Ni and Mn are all in the same row and have similar properties. Although Al is not in the same cycle, at this time, the content of Al is less and the influence is weak. The main phase in the alloy is FCC phase. Continue to increase the content of Al, and the original diffraction peak disappears, at this time at 2θ= New (110), (200) and (211) strong diffraction peaks appear at 45°, 66.5° and 82°, that is, BCC phase (Al Ni solid solution). It can be seen from Table 4 that Al and Ni elements have the most negative mixing enthalpy, so it is easiest to combine to form Al Ni solid solution. The intensity of (110) diffraction peak in Al$_{1.5}$ cladding layer continues to increase, showing all BCC phases.

This shows that the formation of BCC phase is promoted with the increase of Al content. This is mainly caused by the high entropy effect of the high entropy alloy. It can be seen from Table 3 that when the content of Al element gradually increases, the mixing entropy of the alloy increases. The more elements, the greater the mixing entropy of the cladding layer, and there is not enough free energy to make them react with each other to form complex intermetallic compounds, and finally form a simple solid solution phase structure; Therefore, only a single FCC solid solution phase and BCC solid solution phase will be formed in the alloy. At the same time, due to the large radius of Al atom (0.1432nm), the original lattice will be changed, which will enhance the degree of lattice distortion, squeeze into the solid solution of FCC phase structure, and form the solid solution of BCC structure.

3.2. Microstructures of alloys

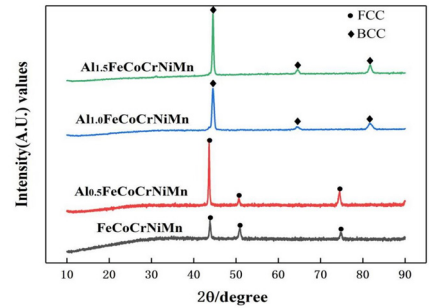The OM results of AlxFeCoCrNiMn high entropy alloy cladding layer and SEM results of Al1.0 cladding layer are

Figure 2. XRD patterns of AlxFeCoCrNiMn cladding layer.

Table 2. The chemical composition of Q345 steel.

Element	C	Mn	Si	P	S
Mass(%)	≤0.2	≤1.7	≤0.5	≤0.035	≤0..035

Table 3. Chemical compositions of AlxFeCoCrNiMn high entropy alloy powder(mass fraction/%).

x	Al	Fe	Co	Cr	Ni	Mn	name
0	-	19.9166	21.0172	18.5433	20.9305	19.5925	Al0
0.5	4.5903	19.0024	20.0525	17.6921	19.9697	18.6931	Al0.5
1.0	8.7777	18.1684	19.1724	16.9156	19.0933	17.8727	Al1.0
1.5	12.6130	17.4045	18.3663	16.2044	18.2905	17.1213	Al1.5

shown in Figure 3. When Al is not added, the microstructure of the cladding layer is mainly composed of dendrites. Al_0 cladding layer is mainly dendrite, $Al_{0.5}$ cladding layer is mainly columnar dendrite, and $Al_{1.0}$ cladding layer forms equiaxed crystal. This shows that equiaxed crystals appear in the microstructure when the content of Al element increases gradually. And some irregular grains will be formed inside and on the grain boundary. The formation of equiaxed crystals is attributed to the characteristics of rapid heating and rapid cooling in laser processing: the laser beam has the characteristics of high energy density, and the higher temperature provides the conditions for phase fluctuation and structure fluctuation during alloy solidification. At this time, a large number of crystal nuclei are generated in the cladding, and the faster cooling rate increases the nucleation rate, thereby forming fine equiaxed crystals. Figure 4 shows the SEM and surface scanning results of $Al_{1.0}$ high entropy alloy cladding layer. The results show that equiaxed grains appear in the structure when Al content increases gradually. The formation of equiaxed grains is attributed to the characteristics of rapid heating and rapid cooling in laser processing: under the action of high energy of laser beam, the alloy powder melts rapidly, and a large number of nuclei are produced in the cladding layer, but the faster cooling rate makes the nuclei do not have enough time to grow and it is difficult to form cell, so the fine equiaxed grains are formed. Figure 5 shows the SEM and surface scanning results of $Al_{1.5}$ cladding layer: however, as the Al element

continues to increase, dendritic cellular crystals appear in $Al_{1.5}$ cladding layer. According to Gibbs free energy law and Boltzmann thermodynamic statistical principle, the mixing entropy increases further, and the lower the free energy, the more stable the alloy system is. When the percentage of each atom is the same, the mixing entropy of the alloy system is the largest.

Therefore, when x = 0, 0.5, 1.0, the mixing entropy of the alloy is the largest, the system is the most stable, no other crystals are formed, mainly equiaxed crystals. When x = 1.5, the mixing entropy decreases and the free energy increases, so that there are more time and space for the interaction between the elements in the system, resulting in the columnar and cellular structures in the microstructure of the cladding layer. In addition, Al atoms are dissolved in the lattice of BCC phase, resulting in solution strengthening.

With the increase of Al content, EDS spectrum shows that, as shown in Table 6, when x = 0 and x = 0.5, the element content in each position of the structure is very uniform, and there is no segregation of components, which is consistent with the XRD results, only a simple FCC solid solution structure is formed, and the proportion of various elements is also consistent with Table 1. When x = 1.0, obvious equiaxed grains are formed, and there are obvious grain boundaries and grain interior in equiaxed grains. Table 6 shows that the increase of Al and Ni in grains leads to the decrease of Ni content at grain boundaries, accompanied by the decrease of Al content, which indicates that the lower enthalpy value

**Table 4.** Mixing enthalpy parameter between binary (KJ/mol).

element	Al	Co	Cr	Fe	Mn	Ni
Al	-	-19	-10	-11	-19	-22
Co	-	-	-4	-1	-5	0
Cr	-	-	-	-1	-2	-7
Fe	-	-	-	-	0	-2
Mn	-	-	-	-	-	-8
Ni	-	-	-	-	-	-

Table 5. Alloy parameter table.

alloy	T_{mix}/K	$\triangle H_{mix}$/J•mol^{-1}•K^{-1}	$\triangle S_{mix}$/J•mol^{-1}•K^{-1}	Ω	δ/%
FeCoNiCrMn	1518.8	-4800	13.38	4.23	2.6
$Al_{0.5}$FeCoNiCrMn	1440.7	-5306	14.70	3.99	3.5
$Al_{1.0}$FeCoNiCrMn	1375.7	-12333	14.90	1.66	5.3
$Al_{1.5}$FeCoNiCrMn	1320.3	-14844	14.78	1.31	6.2
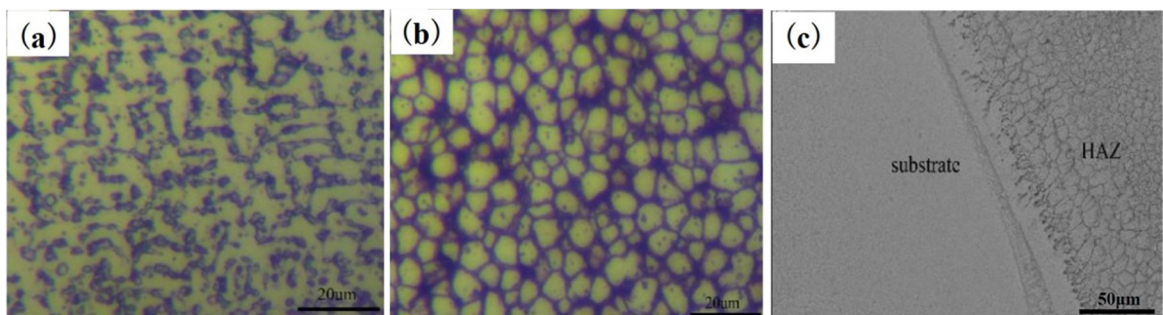
Figure 3. OM and SEM of cladding layer (a) x = 0 (b) x = 1.0 (c) bonding zone between substrate and cladding layer.
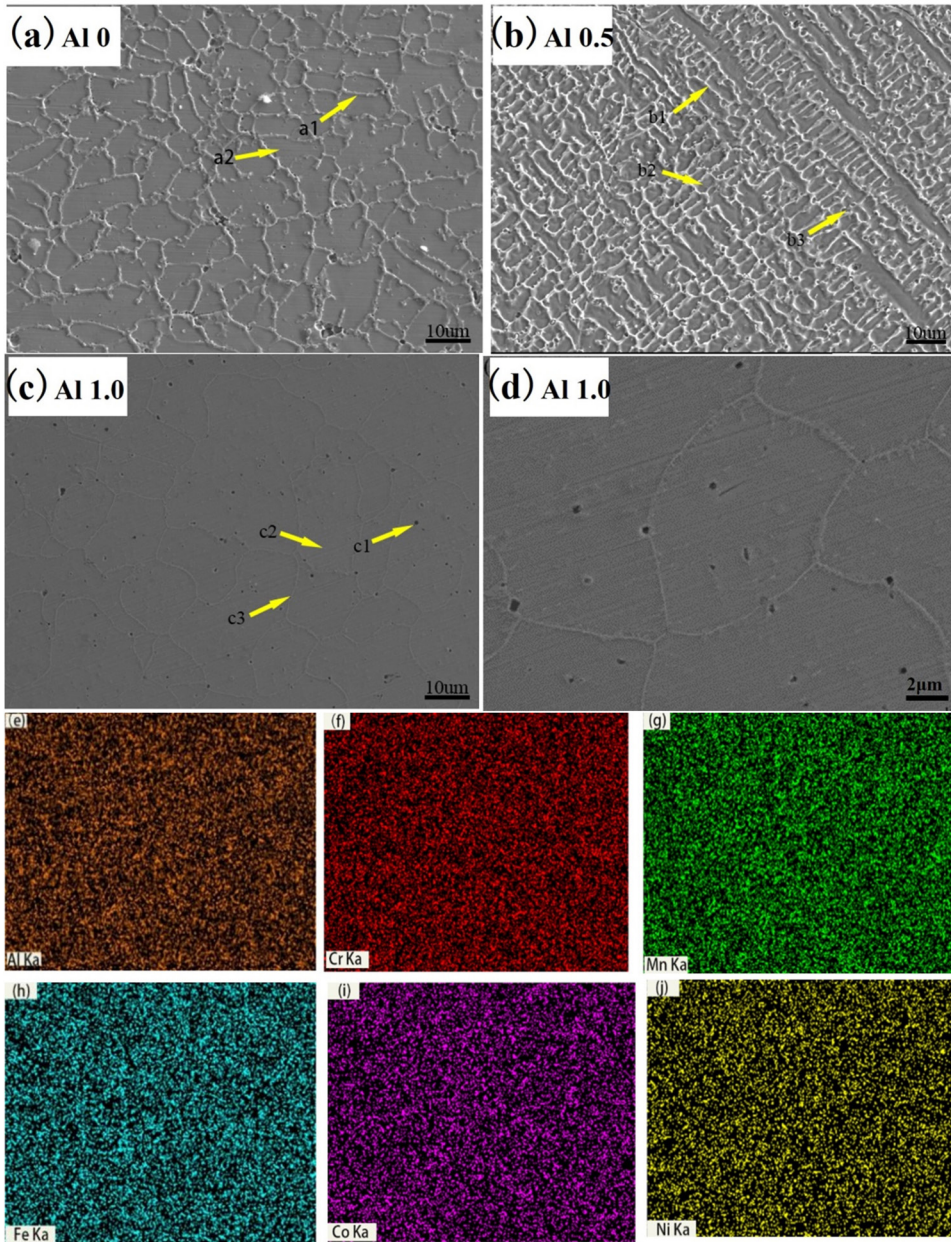
Figure 4. SEM results of cladding layer and surface scanning results of Al1.0 (a) x = 0 (b) x = 0.5 (c) x = 1.0 (d) x = 1.5 (e-j) x = 1.0 cladding laye.
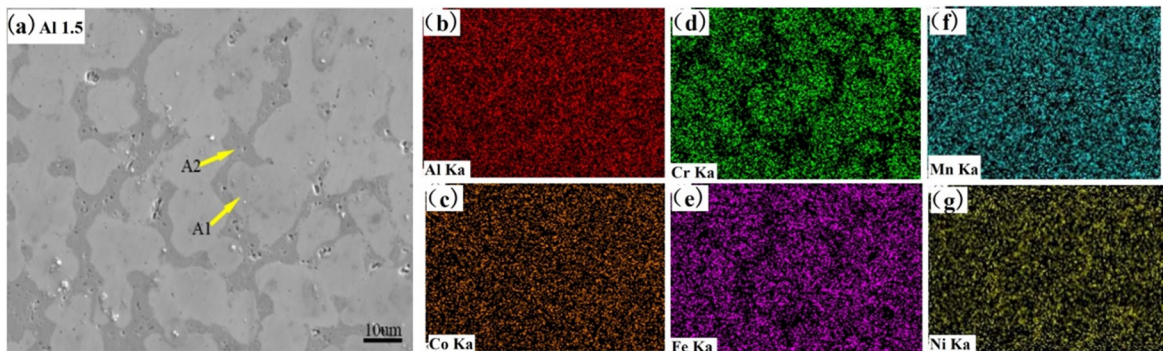
Figure 5. Elementenl distribution of Al1.5 cladding layer.

between Al and other metals ensures that Al atoms have better bonding ability than other atoms. At the same time, Al with large atomic radius is dissolved in the lattice of BCC phase, resulting in lattice distortion and increase of BCC solid solution, which is consistent with XRD results. According to EDS energy spectrum, the content of Al and Ni at the grain boundary increases, resulting in a significant decrease in the content of Ni in the crystal, accompanied by a decrease in the content of Al. According to Table 4, there is a negative enthalpy relationship between Al element and other metal elements. The more negative the enthalpy, the stronger the bonding ability between the two elements. Therefore, the bonding ability of Al atom is better than that of other atoms. The enthalpy between Al and Ni is the minimum of -22kJ/mol, which makes Al and Ni easier to combine and gather at the grain boundary. It leads to the formation of BCC solid solution with Al Ni as matrix, which leads to the increase of Ni and Al content at the grain boundary. In addition, EDS results show that the Fe content in the cladding layer is significantly higher than the theoretical value, which is due to the partial melting of Q345 steel surface into the cladding layer under the action of laser, so the Fe content in the cladding layer increases and other elements are diluted. In addition, the Al content is obviously lower than the actual value, because the melting point of Al element is low, and it is seriously burned under the action of high laser energy. Moreover, during the laser cladding process, Al element is oxidized, resulting in the formation of Al_2O_3 on the surface of the cladding layer, and finally discharged in the form of scum on the surface of the cladding layer, resulting in the lower Al content than the actual value.

3.3. Microhardness of alloys

The average thickness of cladding layer is 5mm, and Figure 6 shows the hardness distribution of AlxFeCoCrNiMn (x=0, 0.5, 1.0, 1.5) high entropy alloy cladding layer. With the increase of Al content, the hardness has been improved to different degrees. When x = 0, 0.5, The microhardness is 1.2 times that of the matrix.The microhardness of the alloy was increased significantly. When x = 1,1.5, the microhardness of the cladding layer can reach 617.9HV,643.9HV, which is nearly three times of the matrix.

It can be seen that the microhardness distribution of Al0.5, Al1.0 and Al1.5 cladding are different, which is caused by

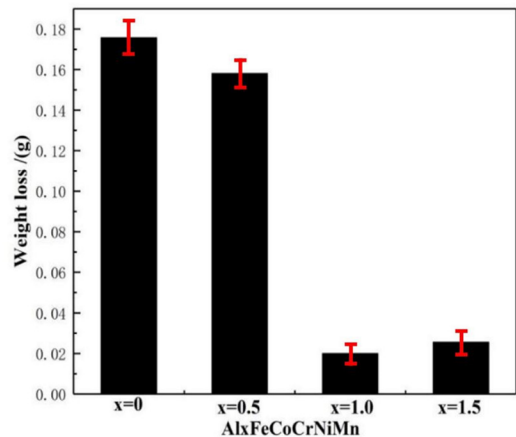the segregation of Al elements and the growth in the crystal. The results of XRD show that the reason for the hardness increase is that the addition of Al promotes the transition of FCC with soft hardness to BCC with higher hardness, and the solid solution strengthening effect is enhanced, and the hardness is improved. In addition, the addition of Al element increases the lattice distortion of solid solution, further enhances the effect of solid solution strengthening and hardness. On the other hand, because of the characteristics of laser rapid solidification, the atoms in the cladding layer cannot be diffused in time, which increases the solid solution limit of the cladding layer, making the nucleation of the grains difficult and difficult to grow, the grains are refined and the hardness is improved.
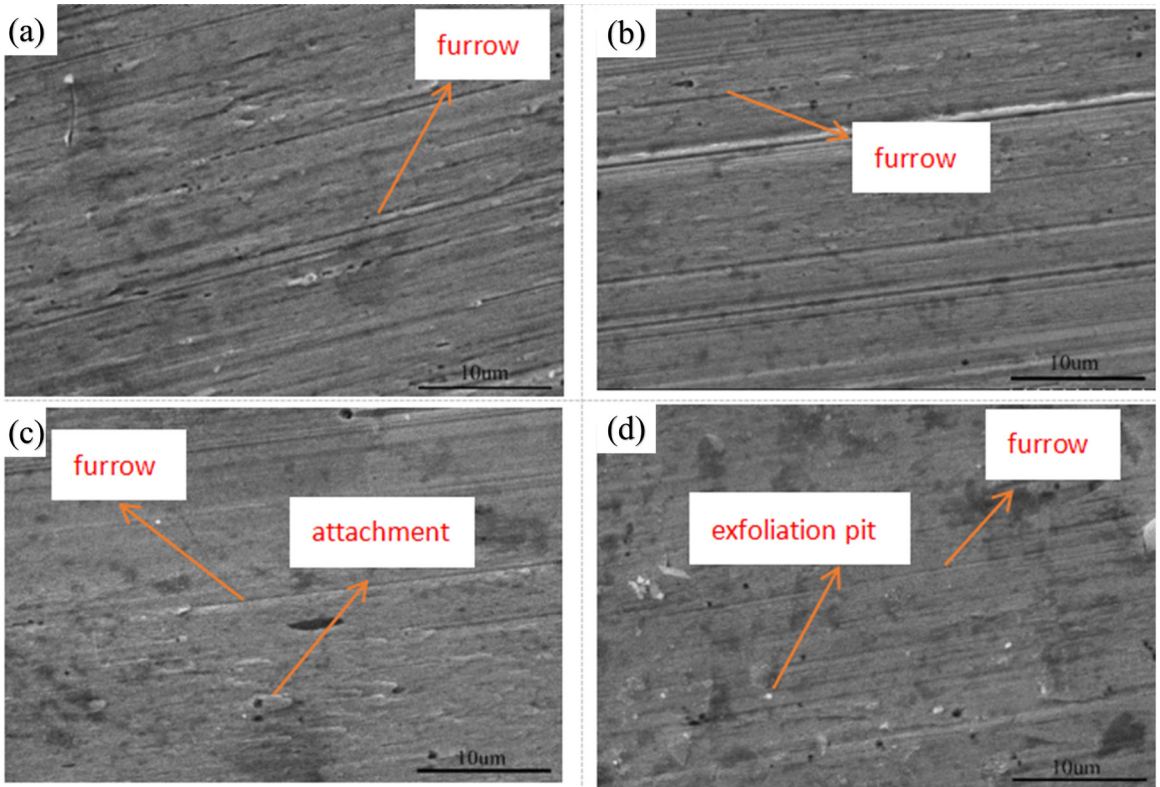
3.4. Wear resistance of alloys

The wear loss of AlxFeCoCrNiMn high entropy alloy is shown in Figure 7. When x = 0 and x = 0.5, the average weight loss is 0.1756mg and 0.1621mg respectively, and the wear loss is relatively large; When x = 1.5, the wear amount is close to 0.0191mg, and the weight loss of wear decreases
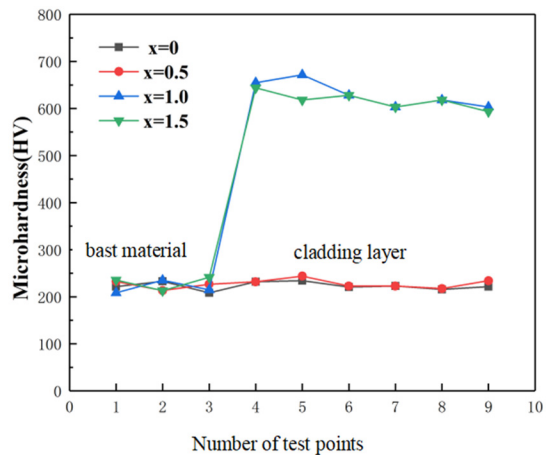
Figure 6. Hardness distribution of AlxFeCoCrNiMn high entropy alloy.

Table 6. Chemical compositions results of AlxFeCoCrNiMn cladding layer (at.%).

Spectrum	Al	Fe	Co	Cr	Ni	Mn
a1	0	20.08	21.91	19.94	19.94	18.13
a2	0	20.50	21.35	19.99	17.05	21.10
b1	3.14	22.46	20.30	19.24	17.81	17.05
b2	3.38	19.34	20.96	17.82	20.84	17.67
b3	2.79	21.10	21.92	19.47	17.75	16.97
c1	21.26	18.93	15.69	18.75	11.41	13.95
c2	5.88	23.13	20.33	20.39	15.51	14.76
c3	2.41	26.37	18.64	29.53	7.47	15.59
A1	10.92	15.01	19.53	12.31	21.60	16.83
A2	3.39	25.21	17.11	24.84	13.21	16.23

Figure 7. Wear loss of AlxFeCoCrNiMn high entropy alloy.

Figure 8. SEM images of worn areas of AlxFeCoCrNiMn cladding layer (a) x=0(b)x=0.5 (c) x=1.0 (d) x=1.5.

obviously, indicating that the wear resistance increases. The trend of wear loss is opposite to that of hardness, which also shows that the higher the hardness is, the higher the wear resistance is. Moreover, with the increase of Al content, the wear resistance of the cladding layer increases. The wear surface is mainly characterized by adhesion, shedding and furrow, as shown in Figure 8. When x = 0, there are parallel grooves and some scratches on the surface of the sample, which are mainly micro wear. When the content of Al continues to increase, obvious furrow appears, accompanied by the appearance of attachments. Obviously, the $Al_{0.5}$ cladding layer is mainly abrasive wear, and $Al_{1.0}$ cladding layer is the mixed mechanism of abrasive wear and adhesive wear. With the increase of Al content, exfoliation pits formed due to exfoliation appear on the surface of $Al_{1.5}$ cladding layer, and there are obvious grooves and shallow cracks on the surface, which indicates that the combined mechanism of abrasive wear and micro cutting is the main one. This may be due to the increasing effect of solution strengthening with the addition of a large amount of Al element, which leads to the crack tendency of $Al_{1.5}$ cladding layer and increases the risk of brittle fracture. The results show that $Al_{1.0}$ coating has better wear resistance.

4. Conclusions

(1) With the increase of Al content, the phase structure of AlxFeCoCrNiMn cladding layer changes from simple FCC solid solution structure to FCC + BCC structure. This is due to the addition of Al atoms into FCC solid solution, resulting in lattice distortion and BCC structure solid solution. The microstructure changes from fine equiaxed crystal to cellular crystal with the increase of Al content. However, the elements are evenly distributed and no intermetallic compound is formed. The hardness of AlxFeCoCrNiMn cladding layer increases with the increase of Al content, and the microstructure hardness of $Al_{1.5}$ cladding layer reaches the maximum.

(2) The wear mechanism of AlxFeCoCrNiMn cladding layer is mainly abrasive wear and adhesive wear, and that of $Al_{0.5}$ cladding layer is mainly abrasive wear; $Al_{1.0}$ cladding layer is a mixed mechanism of abrasive wear and adhesive wear; $Al_{1.5}$ cladding layer is mainly a combined mechanism of abrasive wear and micro cutting. Considering the weight loss and wear mechanism, $Al_{1.0}$ cladding layer has better wear resistance.

6. References

1. Yeh J-W, Chen S-K, Lin S-J, Gan J-Y, Chin T-S, Shun T-T, et al. Nanostructured high-entropy alloys with multiple principal elements: novel alloy design concepts and outcomes. Adv Eng Mater. 2004;6(5):299-303.

2. Pogrebnjak AD, Bagdasaryan AA, Yakushchenko IV, Beresnev VM. The structure and properties of high-entropy alloys and nitride coatings based on them. Russ Chem Rev. 2014;83(11):1027-61.

3. Yue TM, Xie H, Lin X, Yang HO, Meng GH. Solidification behaviour in laser cladding of AlCoCrCuFeNi high-entropy alloy on magnesium substrates. J Alloys Compd. 2014;587:588-93.

4. Yang X, Zhang Y. Prediction of high-entropy stabilized solid-solution in multicomponent alloys. Mater Chem Phys. 2012;132(2-3):233-8.

5. Huang C, Zhang YZ, Vilar R, Shen JY. Dry sliding wear behavior of laser clad TiVCrAlSi high entropy alloy coatings on Ti-6Al-4V substrate. Mater Des. 2012;41:338-43.

6. Shuang S, Ding ZY, Chung D, Shi SQ, Yang Y. Corrosion resistant nanostructured eutectic high entropy alloy. Corros Sci. 2020;164:108315.

7. Lu TW, Feng CS, Wang Z, Liao KW, Liu ZY, Xie YZ, et al. Microstructures and mechanical properties of $CoCrFeNiAl_{0.3}$ high-entropy alloy thin films by pulsed laser deposition. Appl Surf Sci. 2019;494:72-9.

8. Huang KJ, Lin X, Wang YY, Xie CS, Yue TM. Microstructure and corrosion resistance of $Cu_{0.9}NiAlCoCrFe$ high entropy alloy coating on AZ91D magnesium alloys by laser cladding. Mater Res Innov. 2014;18(Suppl 2):S2-1008-11.

9. Huang C, Zhang Y, Shen J, Vilar R. Thermal stability and oxidation resistance of laser clad TiVCrAlSi high-entropy alloy coatings on Ti-6Al-4V alloy. Surf Coat Tech. 2011;206(6):1389-95.

10. Zhang M, Zhou X, Yu X, Li J. Synthesis and characterization of refractory TiZrNbWMo high-entropy alloy coating by laser cladding. Surf Coat Tech. 2017;311:321-9.

11. Cheng J, Liu D, Liang X, Chen Y. Evolution of microstructure and mechanical properties of in situ synthesized TiC-TiB2/CoCrCuFeNi high entropy alloy coatings. Surf Coat Tech. 2015;281:109-16.

12. Shang C, Axinte E, Sun J, Li X, Li P, Du J, et al. CoCrFeNi(W1xMox) high-entropy alloy coatings with excellent mechanical properties and corrosion resistance prepared by mechanical alloying and hot pressing sintering. Mater Des. 2017;117:193-202.

13. Zhang Y, Zuo TT, Tang Z, Gao MC, Dahmen KA, Liaw PK, et al. Microstructures and properties of high-entropy alloys. Prog Mater Sci. 2014;61:1-93.

14. Yu Y, Wang J, Li JS, Kou HC, Liu WM. Characterization of BCC phases in AlCoCrFeNiTix high entropy alloys. Mater Lett. 2015;138:78-80.

15. Zeng P, Li FJ, Sha YY, Chang S, Chai PZ, Liu M. Effect of heat treatment temperature on Microstructure and hardness of AlxCoCrFeNi high entropy alloy. Shanghai Metal. 2020;42:67-71.

16. Bao YY, Ji XL, Ji CC, Zhao JH, Cheng JB, Xu L. Corrosion and erosion resistance of laser cladding FeCrNiCoAlx high entropy alloy coating. Mater Des. 2019;47:141-7.

17. Liu J, Liu H, Chen P, Hao J. Microstructural characterization and corrosion behaviour of AlCoCrFeNiTix high-entropy alloy coatings fabricated by laser cladding. Surf Coat Tech. 2019;361:63-74.

18. Liu H, Liu J, Li X, Chen PJ, Yang HF, Hao JB. Effect of heat treatment on phase stability and wear behavior of laser clad $AlCoCrFeNiTi_{0.8}$ high-entropy alloy coatings. Surf Coat Tech. 2020;392:125758.

19. Cui Y, Shen JQ, Hu SS, Geng K. Oxidation and wear mechanisms of FeCoCrNiMnAlx cladding layers at high-temperature condition. Coatings. 2020;10(11):1136.